Growth Rates of the Principal Facets of Ice between -10 C to -40 C

Kenneth G. Libbrecht[1]

Norman Bridge Laboratory of Physics, California Institute of Technology 264-33, Pasadena, CA 91125

[submitted to the Journal of Crystal Growth, with revisions, August 21, 2002]

Abstract. We describe measurements of the growth rates of the basal and prism facets of ice crystals grown from the vapor phase at temperatures $-39 < T < -10$ C. We find that all our data can be well described by a model in which the facet growth is limited primarily by 2D nucleation over this temperature range. The inferred critical supersaturations, and thus the step edge free energies, are essentially identical for the two facets, with values that decrease monotonically with increasing temperature. The growth scaling parameters, on the other hand, exhibit a more complex behavior with temperature that is quite different for the two facets. These data suggest that much of the peculiar behavior seen in ice crystal growth from vapor is due to differences in the surface diffusion of admolecules on the two principal facets.

1. Introduction

The physical properties of water, its many equilibrium states, and its various phase transitions have been investigated in considerable detail, motivated in part by the importance of water in our environment [1, 2]. Ice crystal growth from the vapor phase is a particularly common phase transition, resulting in the precipitation of copious snow crystals in the atmosphere, yet the basic mechanisms which determine the ice surface growth rates are still only very poorly understood [3, 4]. One of the most puzzling aspects of ice crystal growth from the vapor is that the growth rates exhibit a complex dependence on temperature, which is different for the basal and prism facets. These changing growth rates give rise to the well-known variation of snow crystal morphology with temperature: growth forms in air are plate-like at -2 C, columnar at -5 C, plate-like again at -15 C, and columnar again at -30 C [3]. This unusual temperature behavior has never been explained with certainty, even qualitatively, although it is generally believed that surface melting plays a major role in defining the ice crystal growth rates [3, 4]. Unfortunately surface melting and its role in crystal growth are not well understood theoretically, and in the case of ice even the temperature of the surface melting transition is in some dispute [1].

We believe that an accurate determination of the growth rates of the principal (basal and prism) faces of ice as a function of both temperature and supersaturation could shed light on the dominant growth mechanisms under different conditions. First of all, the growth rate as a function of supersaturation at fixed temperature can indicate the growth mechanism, since different mechanisms generally exhibit different functional dependences on supersaturation. Second, a number of material parameters specific to ice can be derived from growth measurements, once the growth mechanism has been certainly identified. Finally, we believe that a careful study of this system may also guide the development of a detailed theoretical model describing the effects of surface melting on crystal growth in general.

A number of measurements of ice crystal growth rates from the vapor have already been reported in the literature, but to date the measurements have not given consistent results [3–10]. Several of these papers reported measurements of ice crystals growing on substrates under pure water vapor conditions [5–7], similar to what we are reporting here. In each of the latter measurements,

[1] Address correspondence to *kgl@caltech.edu*; URL: http://www.its.caltech.edu/~atomic/

however, the growing ice crystal surfaces typically intersected the substrates upon which the crystals grew. The resulting interaction between the substrate and the growing ice surface may explain the discrepancies between the different data sets, since there is ample evidence that contact between an ice surface and a substrate can greatly alter the growth rate [5, 6, 8]. Free-fall growth experiments eliminate substrate interactions, and thus may yield more reliable measurements [3, 10], although correcting for particle and heat diffusion in such experiments can be very difficult.

We developed a new experimental technique for the present set of measurements which we believe eliminates many of the problems inherent in the previous measurements. Using the procedures described in the next section we were able to grow isolated, oriented, ice crystals on a flat substrate, where the growing facet is parallel to, and thus not intersecting, the substrate. Crystals were grown under nearly pure water vapor conditions, so that particle diffusion in the region above the crystal did not significantly hinder growth. We believe that the current measurements are considerably more reliable than previous attempts, and are thus considerably more useful in trying to understand the enigmatic properties of ice crystal growth from the vapor.

2. Experimental Procedures

The technique we developed combines free-fall growth, which can produce copious numbers of nearly perfect hexagonal prism crystals, with substrate growth, where the growth conditions can be more accurately controlled and the growth rates better monitored. Figures 1 and 2 show schematic views of the crystal growth apparatus used for the measurements presented here. A run began with the free-fall growth chamber (Figure 1) and the secondary chamber (Figures 1 and 2) both held at the same temperature. For measurements of the basal growth rates this temperature was approximately $T_0 = -15$ C, while for measurements of the prism growth rates we had $T_0 = -5$ C. Both chambers contained laboratory air at a pressure of one atmosphere when a run began.

Crystals were nucleated in the free-fall chamber using rapid expansion of saturated nitrogen gas at approximately 40 psi pressure [11]. The pressurized gas spent a considerable time passing through the U-tube shown in Figure 1, and during its passage the gas became chilled to T_0 and saturated by exposure to ice inside the U-tube. When ice crystals were desired, the valves at the end of the U-tube were opened in sequence to first pressurize and then discharge the small chamber between the valves, which had a volume of roughly 30 cm^3.

The minute ice crystals produced by the gas expansion then entered the free-fall chamber, in which heated water reservoirs provided a continuous source of water to supersaturate the air. The ice crystals grew in this environment until they became heavy enough to begin to drift downward under the influence of gravity. This took roughly one minute, and produced crystals that were typically 5-20 μm in size by the time they reached the bottom of the free-fall chamber. At $T_0 = -15$ C these crystals were typically in the form of thin plate-like hexagonal prisms, while at $T_0 = -5$ C the crystals grew into slender columnar hexagonal prisms.

At the end of the free-fall growth phase some of the crystals were transferred to the secondary chamber via a valved transfer tube (Figure 1). A vacuum pump was used to draw air slowly from the free-fall chamber to the secondary chamber, bringing small ice crystals with it. The air flow was controlled using a needle valve in the vacuum line, and with the transfer valve. The transfer process was repeated until one, or at most a few, crystals fell by chance onto the growth substrate (Figure 2), which was made from an anti-reflection-coated BK-7 glass window with a clear aperture of three millimeters. The crystals were large enough that plate-like crystals usually fell with one basal facet in contact with the substrate, and columnar crystals usually fell with one prism facet in contact with the substrate. We found that the crystal transfer process only worked well if the two chambers were at nearly the same temperature.

High-resolution optical microscopy was used to examine the crystals as they fell onto the substrate, and only nearly ideal crystals were chosen for subsequent measurements. If a crystal morphology was not that of a simple hexagonal prism, or if it had nearby neighboring crystals, or if its

orientation relative to the substrate was not adequate, then the crystal was quickly discarded by heating the substrate slightly. We found that "cycling" the growth of a crystal – growing it, then sublimating it back down, then growing it again – often yielded crystals with non-ideal morphologies. Therefore for the measurements presented here the crystals were grown just once, and not subsequently cycled.

An ice-coated copper disk inside the secondary chamber served as a water vapor source for subsequent growth of crystals on the substrate (Figure 2). It was covered with ice at the beginning of each experimental run, and the source/substrate temperature difference, $\Delta T = T_{source} - T_{substrate}$, was carefully controlled using a pair of matched thermistors mounted on the two surfaces. Both T_{source} and $T_{substrate}$ were controlled using separate thermoelectric modules, and the walls of the secondary chamber were kept at a temperature $T_{chamber}$ about two degrees higher than T_{source}.

After the crystal transfer process we then changed the temperature of the secondary growth chamber to the final target temperature. This took as long as 30 minutes (for the maximum temperature change, going from $T_{chamber} = T_0 = -5$ C to $T_{chamber} = -39$ C), during which time the chosen crystal rested on the substrate and the chamber remained filled with air. The crystal was monitored optically during the temperature change, and ΔT was adjusted frequently to keep the crystal from either growing or shrinking. Once the target temperature was reached, the air was pumped slowly out of the secondary chamber, typically to a base pressure of 2-4 Torr.

Growth of the top crystal facet, with a growth direction perpendicular to the substrate, was measured using optical interferometry between the two ice facets that were parallel to the substrate. (see Figures 1 and 2). A Helium-Neon laser was focused to a roughly 4-μm spot size on the crystal using the same microscope objective used for the imaging system. Laser light reflecting off the two crystal faces was imaged as a bright spot on the crystal, and interference caused the spot to change in brightness as the crystal grew. An interferometer "fringe", or complete brightness cycle, corresponded to a thickness change of $\Delta t = \lambda/2n = 243$ nm, where $\lambda = 633$ nm is the laser wavelength and $n = 1.3$ is the index of refraction of ice. Note that the laser power was low, so crystal heating by the laser was completely negligible. From direct optical imaging we also monitored "lateral" growth of the crystals (i.e. growth along directions parallel to the substrate), although these measurements were not used in the analysis presented below.

Our absolute measurements of T_{source} and $T_{substrate}$ were not accurate enough to directly determine ΔT to the level necessary in these experiments. Thus once the growth chamber had stabilized at its final temperature and pressure, we calibrated ΔT by warming the substrate slowly until the crystal began to sublimate. Once the zero for ΔT was established in this way, $T_{substrate}$ was slowly reduced, which increased ΔT and caused the crystal to grow. Typically ΔT was increased slowly, so that growth measurements with a given crystal were first performed at low ΔT, when the crystal size was small. For each growth run the crystal image was continuously recorded on videotape along with ΔT, and the interference fringes were counted during playback to determine the crystal growth velocity v as a function of ΔT.

3. Growth Rate Measurements and Parameterization

The raw data from each growth run gave the growth velocity v of a single crystal facet as a function of ΔT. The background gas pressure was low enough that particle diffusion above the crystal did not substantially hinder the crystal growth (see the Appendix below). Thus we can convert ΔT to surface supersaturation using

$$\sigma = \frac{1}{p_{sat}} \frac{dp_{sat}}{dT} \Delta T \tag{1}$$

where p_{sat} is the equilibrium vapor pressure of ice. We then write the growth velocity in terms of the usual Hertz-Knudsen formula as

$$v = \alpha \frac{\Omega(p - p_{sat})}{\sqrt{2\pi m k T}} \tag{2}$$

$$= \alpha v_{kin} \sigma$$

where p is the water vapor pressure above the growing surface and Ω is the molecular volume. This defines the kinetic velocity v_{kin} and the usual condensation coefficient α (see the Appendix), for which we must have $\alpha \leq 1$. With these relations we convert $v(\Delta T)$ to $\alpha(\sigma)$, and use the latter function in our subsequent analysis.

Figures 3-6 show our measurements of the growth of basal and prism facets at different temperatures. We found that in all cases the data were well described by a model in which the growth is limited primarily by 2D nucleation on the ice surface [12, 14, 15]. This can be readily seen by plotting α versus $1/\sigma$ on a semilog plot [14], and these plots are shown in Figures 5 and 6. We fit the data to the functional form $\alpha(\sigma) \rightarrow A \exp(-\sigma_0/\sigma)$ to produce the two constants A and σ_0 for each measured temperature and for each facet, and these fit parameters are shown in Figure 7.

We see from all these data that the crystal-to-crystal variation was reasonably low, producing a fairly small scatter in all the plots. We observed a systematic downward shift of the high-σ data points at $T = -10$ C, which we believe resulted from crystal heating. As we see from the Appendix (eqn. 32), heating problems are more severe at higher growth temperatures, and as described in the previous section the high-σ data points were taken last, when the crystal sizes were largest. These high-σ points were not included in the fits to the data shown in the figures.

4. Systematic Errors

As mentioned above, previous reported measurements of ice crystals growing on substrates under pure water vapor conditions, similar to what we are reporting here, produced conflicting results [5–7]. From this we must conclude that systematic errors may have affected the different measurements, and we should therefore examine possible systematic effects carefully.

Substrate Interactions. The first potential systematic effect concerns the interaction of a growing ice crystal facet and the growth substrate, as was mentioned earlier. This appears to be an important effect, as several earlier workers have reported evidence that contact between an ice surface and a substrate can substantially alter the growth rates [5,6,8]. From our lateral growth rate measurements we too found a number of unusual growth characteristics for those ice surfaces that intersected the substrate. For example, we regularly observed that the prism facets on plate-like crystals with one basal surface lying on the substrate grew more slowly than those same surfaces grew during free-fall growth at $T_{substrate} = -15$ C. With columnar crystals we occasionally observed that one basal facet was growing rapidly while the other grew much more slowly. We have not yet completely investigated these trends, but our observations support the hypothesis that substrate interactions can distort ice crystal growth data. The data presented here, however, pertain only to the growth of ice surfaces that were not in contact with the substrate. Thus the present data should be free of this systematic effect, in contrast to previous measurements.

Residual Gas Pressure. Referring to eqn. 13 in the Appendix, we grew crystals with $R \approx 10$ μm and $D/D_{air} \approx 0.005$. Under these conditions α_{diff} is sufficiently large that bulk diffusion does not substantially limit the crystal growth rates. Any direct influences of the residual gas on α are also expected to be small at these low pressures [16, 17].

Crystal heating. This is discussed in the Appendix (eqn. 32), and we see that it may limit the growth of larger crystals at higher temperatures. We largely avoided this problem by growing small crystals, typically no more than 10 microns in thickness. We believe heating did influence the high-σ data points at $T = -10$ C, as was described above.

Interference from Neighboring Crystals. As discussed in the Appendix below, performing these measurements at low background gas pressure insures that the growth is limited primarily by attachment kinetics, and not by particle diffusion through the background gas. There is one circumstance, however, for which this argument does not apply. If many crystals grow simultaneously on the substrate, and if some crystals grow in non-faceted forms, then the growth of the faceted crystals is hindered even with a low background pressure. This is so because while the diffusion coefficient is

large at low pressures, it is not effectively infinite until the particle mean-free-path is large compared to the characteristic crystal size or separation between crystals. With a finite diffusion constant the fast-growing non-faceted crystals produce a supersaturation boundary condition of $\sigma \approx 0$ on their fast-growing surfaces. This boundary condition pulls σ down near the faceted crystal, and thus hinders its growth. We avoided this circumstance by making measurements of only very isolated crystals. Also, for our measured crystals the lateral growth velocities were never much higher than the velocity of the parallel facet being measured interferometrically.

Interference from Other Facets. Finally, we note throughout this paper we have assumed that the growth of a particular facet is not influenced by the growth of neighboring facets (except via particle diffusion outside the crystal, which was typically not a substantial factor in the present work). Put another way, we have assumed that admolecules on one facet do not diffuse onto other facets to a significant degree. Our main justification of this assumption is theoretical: surface tension rounds the edges between facets, which are thus expected to be atomically rough, and admolecules are thought to be readily incorporated onto rough surfaces. Another justification of this assumption is that in all cases the measured facets were larger than the other facets, owing to the geometry of the crystals. There is at least one bit of evidence that surface diffusion around corners is possible [12], so this assumption may in fact not be a valid one. If it does not hold then the conclusions we obtain below may be compromised, at least to some degree, owing to the peculiar lateral growth behavior we observed for facets that intersected the substrate.

5. Discussion

Our primary result is that our ice growth data are well represented by the functional form $\alpha(\sigma) = A\exp(-\sigma_0/\sigma)$ over the temperature range $-10 < T < -40$ (for fairly low σ) and from our data we extracted the measured functions $A(T)$ and $\sigma_0(T)$ shown in Figure 7. This functional form is expected when the attachment kinetics is governed by 2D nucleation, and in this case the edge free energy β can be obtained from σ_0 using the relation [12–15]

$$\sigma_0 = \frac{\pi\beta^2\Omega_2}{3k^2T^2} \tag{3}$$

where Ω_2 is the area of a molecule on the surface. Figure 8 shows the edge free energy of a growing ice nucleus as derived from our measurements..

Surprisingly, we found no significant differences in σ_0 between the basal and prism facets over the observed temperature range. This is essentially opposite the conclusion reached by Nelson and Knight [8], who found very different critical supersaturations on different facets, at least near $T = -15$ C where the two data sets overlap. Their experiments, however, were done using large crystals grown in air at a pressure of one atmosphere, where it is especially difficult to compensate for the effects of diffusion on growth, particularly when all the facets are not growing at the same rate (see the Appendix below). We believe the present data, using much smaller crystals grown in a low-pressure environment, are more reliable.

Equally surprisingly, we observed that σ_0 does not show any abrupt behavior near $T = -15$ C, where there are big changes in the relative growth rates of the basal and prism facets [3]. Our measurements of $A(T)$, however, do show a substantial difference between crystal facets, with the rather unusual temperature dependence seen in Figure 7. The low value of A for the basal facet at $T = -15$ C reflects the slow growth of that facet at that temperature, an observation that is consistent with the growth of thin plate-like snow crystals under atmospheric conditions at $T = -15$ C [3].

The decreasing edge free energy of ice for increasing temperatures is vaguely similar to what is seen in the crystal growth of hcp ^{4}He [21]. In the latter system the decrease in the edge free energy is related to the onset of the surface roughening transition, at which point the edge free energy goes to zero. For ice we have to contend with surface melting in addition to possible surface roughening, and the theory is not nearly as well developed as for the helium case. Nevertheless it is plausible

that the observed trend in σ_0 for ice is due to a related physical mechanism.

The abrupt change in dA_{basal}/dT occurring near $T = -15$ C may be related to the surface melting transition, which has been found at nearly this temperature for the basal facet [18] (although this temperature is disputed by other measurements [1]). If we assume the onset of surface melting does occur near $T = -15$ C on the basal facet, then from our observations we would conclude that A_{basal} decreases with increasing temperature below the surface melting transition, which is likely due to changes in the surface transport of admolecules for $T < -15$ C. Above the surface melting transition the ice surface is covered with a substantial quasi-liquid layer, so the molecular dynamics governing the motion of growth steps could be substantially different than below the transition. Thus in this interpretation the behavior of A_{basal} includes a monotonic trend at low temperatures, leading to a sharp decrease near the surface melting transition, followed by an abrupt change once the quasiliquid layer becomes appreciable. Why A_{prism} shows much weaker trends with temperature in comparison with A_{basal} remains a mystery.

Ignoring the complex questions associated with crystal growth in the presence of surface melting, we can still examine the observed trend in $A_{basal}(T)$ for $T < -15$ C, where it is generally believed there is little or no surface melting. For simple growth from the vapor phase, A is related to the surface diffusion constant and the mean lifetime of admolecules on the surface [14]. As the surface melting transition is approached from lower temperatures, our data suggest that either the mean admolecule lifetime or the surface diffusion constant decreases rapidly on the basal surface. Surface diffusion via long jumps has been observed in some metallic systems [19], and an unusually high surface mobility on the ice surface has been inferred from electron and helium scattering even at quite low temperatures [20]. Thus we conclude that anomalous surface diffusion is the most likely explanation of $A_{basal}(T)$ for $T - 15$ C. In this case we speculate that the anomalously high surface diffusion at lower temperatures is frustrated by surface processes associated with the onset of surface melting. Additional work will be needed to further elucidate these processes.

6. Appendix – Considerations From Spherical Growth

The growth of faceted ice crystals from the vapor can be influenced by attachment kinetics at the crystal surface, particle diffusion through any background gas, and crystal heating caused by the condensing vapor. In order to weigh the relative importance of these various influences, it is instructive to consider the growth of a fictitious "faceted" spherical crystal in which we treat the growing surface as if it were atomically smooth. The spherical approximation describes the growth of isometric faceted prisms fairly well (provided all facets have the same physical properties), and we will see below it is useful in other circumstances as well. Some parts of this formalism have previously been described by Yokoyama and Kuroda [22].

6.1 Finite Kinetics, Without Heating

Particle transport through the gas above the crystal is described by the diffusion equation

$$\frac{\partial c}{\partial t} = D\nabla^2 c \tag{4}$$

where $c(r)$ is the particle concentration surrounding the crystal and D is the diffusion constant. We will first ignore latent heat deposition, so temperature is constant throughout the system, and work in terms of the supersaturation level

$$\sigma(r) = \frac{[c(r) - c_{sat}]}{c_{sat}} \tag{5}$$

where c_{sat} is the equilibrium concentration above a flat ice surface. Under essentially all realistic conditions the growth is slow enough that the diffusion equation reduces to Laplace's equation

$\nabla^2\sigma = 0$, which for the spherical case has the simple solution

$$\sigma(r) = A + \frac{B}{r} \tag{6}$$

where the constants A and B are determined by the boundary conditions. We will assume a sphere of radius R growing inside a large sphere of radius $r_{outer} \to \infty$, so that the outer boundary condition gives $A = \sigma_\infty$.

The growth velocity is given by

$$v = \frac{c_{sat} D}{c_{solid}} \frac{d\sigma}{dr}(R) \tag{7}$$

which defines the inner boundary condition. In subsequent calculations we will ignore the Gibbs-Thomson mechanism, in which the equilibrium vapor pressure depends on the radius of curvature of the surface. This is a valid assumption because for most faceted crystals growing from the vapor the effects of attachment kinetics are nearly always much greater than the effects of the Gibbs-Thomson mechanism [23].

We write the growth velocity in terms of the Hertz-Knudsen formula to give

$$v = \alpha v_{kin} \sigma_{surf} \tag{8}$$

where α is the condensation coefficient, $\sigma_{surf} = \sigma(R)$, and the kinetic velocity is

$$v_{kin} = \frac{c_{sat}}{c_{solid}} \sqrt{\frac{kT}{2\pi m}} \tag{9}$$

Combining the two expressions for v gives the mixed boundary condition at the inner radius

$$\frac{d\sigma}{dr}(R) = \frac{c_{solid}}{c_{sat} D} \alpha v_{kin} \sigma(R) \tag{10}$$

and the solution of the diffusion equation gives the growth velocity

$$\begin{aligned} v &= \frac{\alpha \alpha_{diff}}{\alpha + \alpha_{diff}} v_{kin} \sigma_\infty \\ &= \frac{\alpha}{\alpha + \alpha_{diff}} \frac{c_{sat} D \sigma_\infty}{c_{solid} R} \end{aligned} \tag{11}$$

where

$$\begin{aligned} \alpha_{diff} &= \frac{c_{sat} D}{c_{solid} v_{kin} R} \\ &= \frac{D}{R} \sqrt{\frac{2\pi m}{kT}} \end{aligned} \tag{12}$$

In the limit $\alpha_{diff} \ll \alpha$ the growth velocity becomes $v = c_{sat} D \sigma_\infty / c_{solid} R$, which describes diffusion limited growth with fast kinetics, while in the opposite limit we have $v = \alpha v_{kin} \sigma_\infty$, which is valid for kinetics limited growth. For the case of ice growing at $T = -15$ C in air we have

$$\alpha_{diff}(-15C) \approx 0.15 \left(\frac{1\ \mu\text{m}}{R} \right) \left(\frac{D}{D_{air}} \right) \tag{13}$$

where $D_{air} \approx 2 \times 10^{-5}$ m^2/sec is the diffusion constant for water vapor in air at a pressure of one atmosphere.

By writing the growth velocity in this form it becomes apparent that one simply cannot use measurements of the growth velocity v to determine α if $\alpha \gtrsim \alpha_{diff}$. In this case the growth is mostly diffusion limited, and small errors in the determination of v can result in large errors in the derived α. To measure α we must either use very small crystals or reduce the background gas pressure (typically $D \sim P^{-1}$, where P is the background pressure).

6.2 Fast Kinetics, With Heating

Diffusion-limited growth from the vapor is actually a double diffusion problem, since in principle we must consider both particle diffusion to the growing crystal and thermal diffusion to remove the heat generated by condensation at the solid/vapor interface. The spherical case can again be solved exactly in the slow-growth limit. Assuming latent heat is carried away by thermal diffusion only,

the temperature distribution $T(r)$ must be a solution of Laplace's equation, which means we have

$$T(r) = T_\infty + \frac{R\Delta T}{r} \tag{14}$$

where $\Delta T = T_{surf} - T_\infty$. The heat flowing away from the growing sphere is

$$\frac{dQ}{dt} = 4\pi\kappa R\Delta T \tag{15}$$

where κ is the thermal conductivity of the solvent gas, equal to ≈ 0.025 W m^{-1} K^{-1} for air.

The heat flowing out must equal the heat flowing in, which is

$$\begin{aligned} \frac{dQ}{dt} &= \lambda\frac{dM}{dt} \\ &= \lambda\rho v 4\pi R^2 \end{aligned} \tag{16}$$

where λ is the latent heat for the vapor/solid transition ($\lambda_{ice} = 2.8 \times 10^6$ J/kg) and ρ is the solid density ($\rho_{ice} = 917$ kg/m^3), so we have

$$\Delta T = \frac{vR\lambda\rho}{\kappa} \tag{17}$$

To see how the temperature change affects the growth, we have the growth velocity

$$v = \frac{c_{sat}}{c_{solid}}\frac{D}{R}\Delta\sigma \tag{18}$$

where $\Delta\sigma = \sigma_\infty - \sigma_{surf}$, which is valid in the presence of heating. For the case of heating with fast kinetics we have

$$c(R) \approx c_{sat} + \frac{dc_{sat}}{dT}\Delta T \tag{19}$$

where our convention is that c_{sat} is evaluated at T_∞. Putting all this together yields the growth velocity

$$v = \frac{D}{R}\frac{c_{sat}}{c_{solid}}\frac{\sigma_\infty}{1+\chi_0} \tag{20}$$

where

$$\chi_0 = \frac{\eta D\lambda\rho}{\kappa}\frac{c_{sat}}{c_{solid}} \tag{21}$$

with $\eta = d\log(c_{sat})/dT$. Typical values for these parameters are

$T(C)$	c_{sat}/c_{solid}	$v_{kin}(\mu$m/sec)	η	χ_0
-39	0.16×10^{-6}	20	0.11	0.04
-30	0.43×10^{-6}	57	0.10	0.09
-20	0.97×10^{-6}	132	0.096	0.19
-15	1.51×10^{-6}	207	0.092	0.29
-10	2.34×10^{-6}	325	0.088	0.42
-5	3.53×10^{-6}	494	0.086	0.62
-2	4.52×10^{-6}	637	0.083	0.77

where χ_0 is evaluated in air at a pressure of one atmosphere. We see that the main effect of heating on diffusion-limited growth is to scale the growth by a factor of $(1+\chi_0)^{-1}$.

If the diffusion constant is large, so that $\chi_0 \gg 1$, then the growth velocity becomes limited by heating and we have

$$\begin{aligned} v &\approx \frac{\kappa}{\lambda\rho\eta}\frac{\sigma_\infty}{R} \\ &\approx (100\ \mu\text{m/sec})\left(\frac{1\ \mu\text{m}}{R}\right)\sigma_\infty \end{aligned} \tag{22}$$

6.3 Finite Kinetics, With Heating

For the most general case of finite kinetics in addition to heating the analysis is similar to the above,

and the final result is

$$v = \frac{\alpha}{\alpha(1+\chi_0)+\alpha_{diff}} \frac{c_{sat} D \sigma_\infty}{c_{solid} R} \tag{23}$$

If the diffusion constant is large, this becomes

$$v = \frac{\alpha \alpha_{cond}}{\alpha + \alpha_{cond}} v_{kin} \sigma_\infty \tag{24}$$

where

$$\begin{aligned} \alpha_{cond} &= \frac{\kappa}{\eta R \lambda \rho v_{kin}} \\ &\approx 0.5 \left(\frac{1\ \mu\text{m}}{R} \right) \end{aligned} \tag{25}$$

where the latter expression is for growth in air at $T = -15$ C (note κ is roughly independent of background pressure down to low pressures).

6.4 Substrate Simulation

We can use the spherical solution to also examine growth on a substrate if we assume a hemispherical crystal with the flat surface held at the substrate temperature $T_{substrate}$. Then the heat flow into the substrate is approximately

$$\frac{dQ}{dt} \approx \pi G R \kappa_{ice} \Delta T' \tag{26}$$

which gives

$$\Delta T' = \frac{2 \lambda \rho v R}{G \kappa_{ice}} \tag{27}$$

where $G \approx 1$ is a geometric correction and here $\Delta T' = T_{surf} - T_{subst}$. Since $\kappa_{ice}/\kappa_{air} \approx 100$ this reduces the temperature increase by a factor of $\sim$100 when compared to growth in air.

The analysis is again similar to the above, and gives the growth velocity in the general case

$$v = \frac{\alpha}{\alpha(1+\chi_0')+\alpha_{diff}} \frac{c_{sat} D \sigma_0}{c_{solid} R} \tag{28}$$

where

$$\chi_0' = \frac{2 \eta D \lambda \rho}{G \kappa_{ice}} \frac{c_{sat}}{c_{solid}} \tag{29}$$

In the case of fast diffusion this becomes

$$v = \frac{\alpha \alpha_{cond}'}{\alpha + \alpha_{cond}'} v_{kin} \sigma_0 \tag{30}$$

with

$$\alpha_{cond}' = \frac{G \kappa_{ice}}{2 \eta R \lambda \rho v_{kin}} \tag{31}$$

and at $T = -15$ C this gives

$$\alpha_{cond}' \approx 25 G \left(\frac{1\ \mu\text{m}}{R} \right) \tag{32}$$

Note that v_{kin} increases fairly strongly with temperature, so that heating is more likely to limit the growth at higher temperatures.

7. References

[1] V. F. Petrenko and R. W. Whitworth, *Physics of Ice* (Oxford University Press: Oxford) (1999).
[2] P. V. Hobbs, *Ice Physics* (Clarendon Press: Oxford) (1974).
[3] T. Kobayashi and T. Kuroda, in *Morphology of Crystals*, Part B (I. Sunagawa, ed.) (Terra Scientific: Tokyo) (1987).
[4] J. Nelson, *Phil. Mag. A* **81**, 2337 (2001).
[5] D. Lamb and W. D. Scott, *J. Cryst. Growth* **12** (1972) 21.
[6] W. Beckmann and R. Lacmann, *J. Cryst. Growth* **58** (1982) 433.

[7] T. Sei and T. Gonda, *J. Cryst. Growth* **94** (1989) 697.
[8] J. Nelson and C. Knight, *J. Atmos. Sci.* **55** (1998) 1452.
[9] Y. Furukawa and S. Kohata, *J. Cryst. Growth* **129** (1993) 571.
[10] K. G. Libbrecht and H. Yu, *J. Cryst. Growth* **222** (2001), 822.
[11] T. C. Foster and J. Hallett, *J. Appl. Meteor.* **32** (1993) 716.
[12] A. A. Chernov, *Modern Crystallography III* (Springer-Verlag: Berlin) (1984).
[13] E. Yokoyama and T. Kuroda, *J. Meteor. Soc. Japan*, **66** (1988) 927.
[14] Y. Saito, *Statistical Physics of Crystal Growth* (World Scientific: Singapore) (1996).
[15] I. V. Markov, Crystal Growth for Beginners (World Scientific: Singapore) (1995).
[16] W. Beckmann, *J. Cryst. Growth* **58**, 443 (1982).
[17] T. Kuroda and T. Gonda, *J. Meteor. Soc. Japan* **62** (1984) 563.
[18] H. Dosch, A. Leid, and J. H. Bilgram, *Surf. Sci.* **327** (1995) 145.
[19] D. C. Senft and G. Ehrlich, *Phys. Rev. Lett.* **74**, 294 (1995).
[20] J. Braun et al., *Phys. Rev. Lett* **80** (1998) 2638.
[21] P. E. Wolf et al., *J. Phys.* **46** (1985) 1987.
[22] E. Yokoyama and T. Kuroda, *Phys. Rev. A* **41** (1990) 2038.
[23] K. G. Libbrecht, T. Crosby, and M. Swanson, to appear in the J. Cryst. Growth (2002).

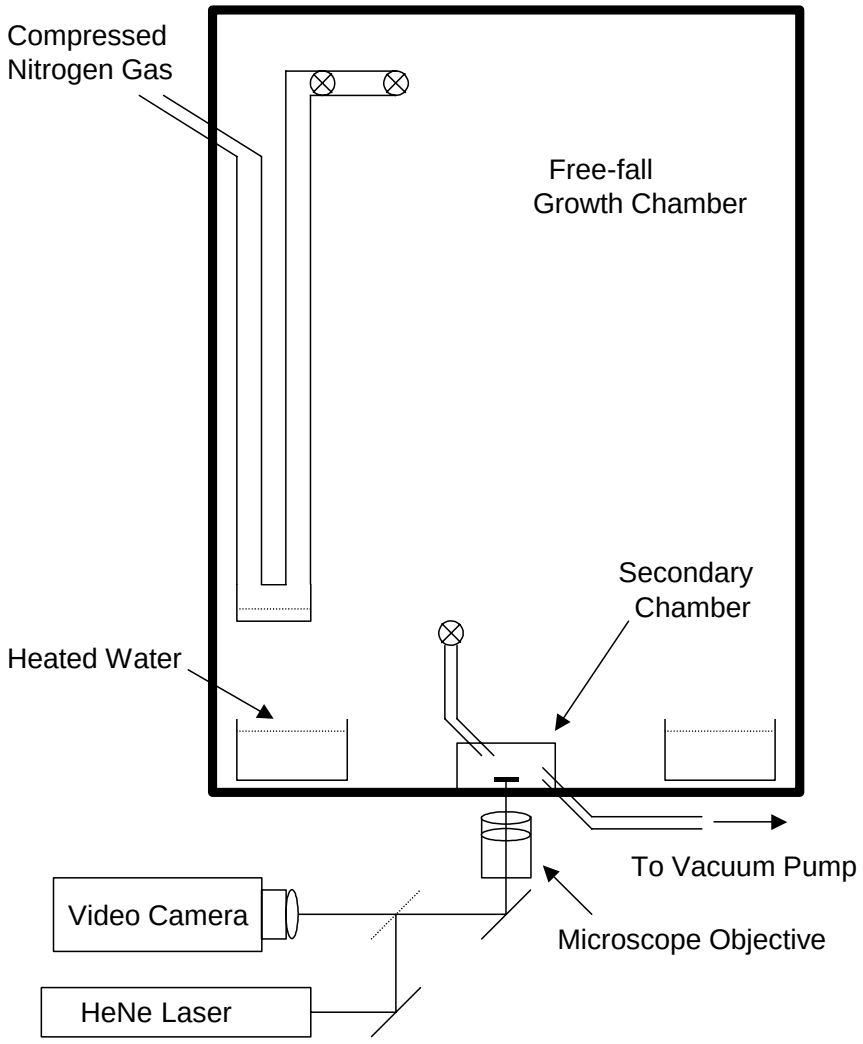

Figure 1. Schematic diagram of the free-fall and secondary growth chambers used in our measurements. Crystals were nucleated and grown in the larger free-fall chamber, and then transfered to a substrate in the secondary chamber for growth measurements. Laser interferometry between the crystal facets was used to measure changes in the crystal thickness as it grew.

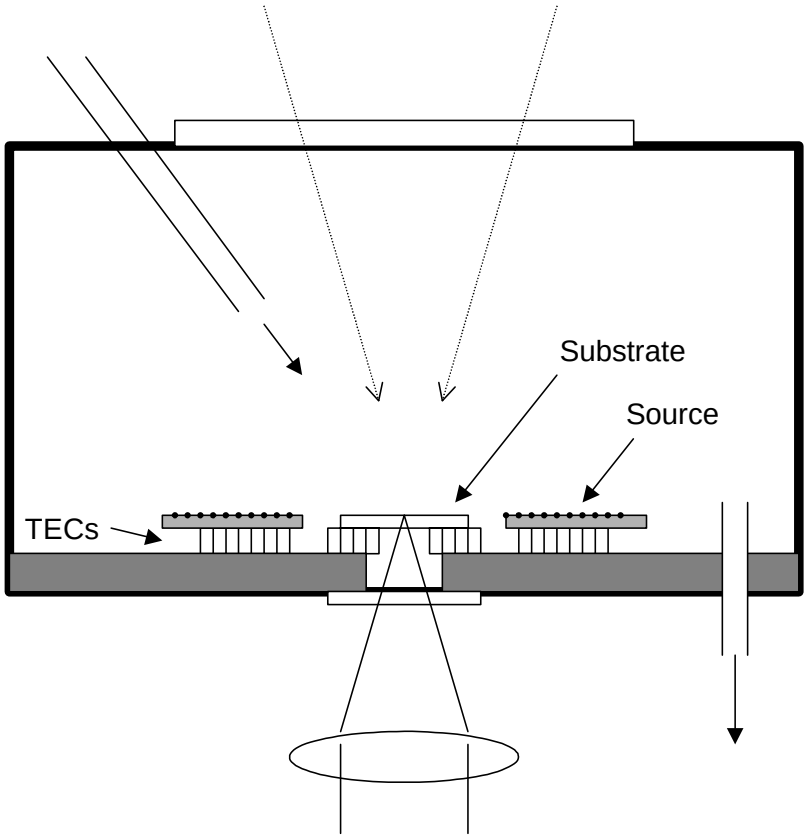

Figure 2. Schematic diagram of the secondary growth chamber used in our measurements. Individual crystals were transferred the substrate, and the chamber was then evacuated. The temperature difference between the substrate and ice-covered source determined the water vapor supersaturation. The crystal was illuminated from above, and imaged from below.

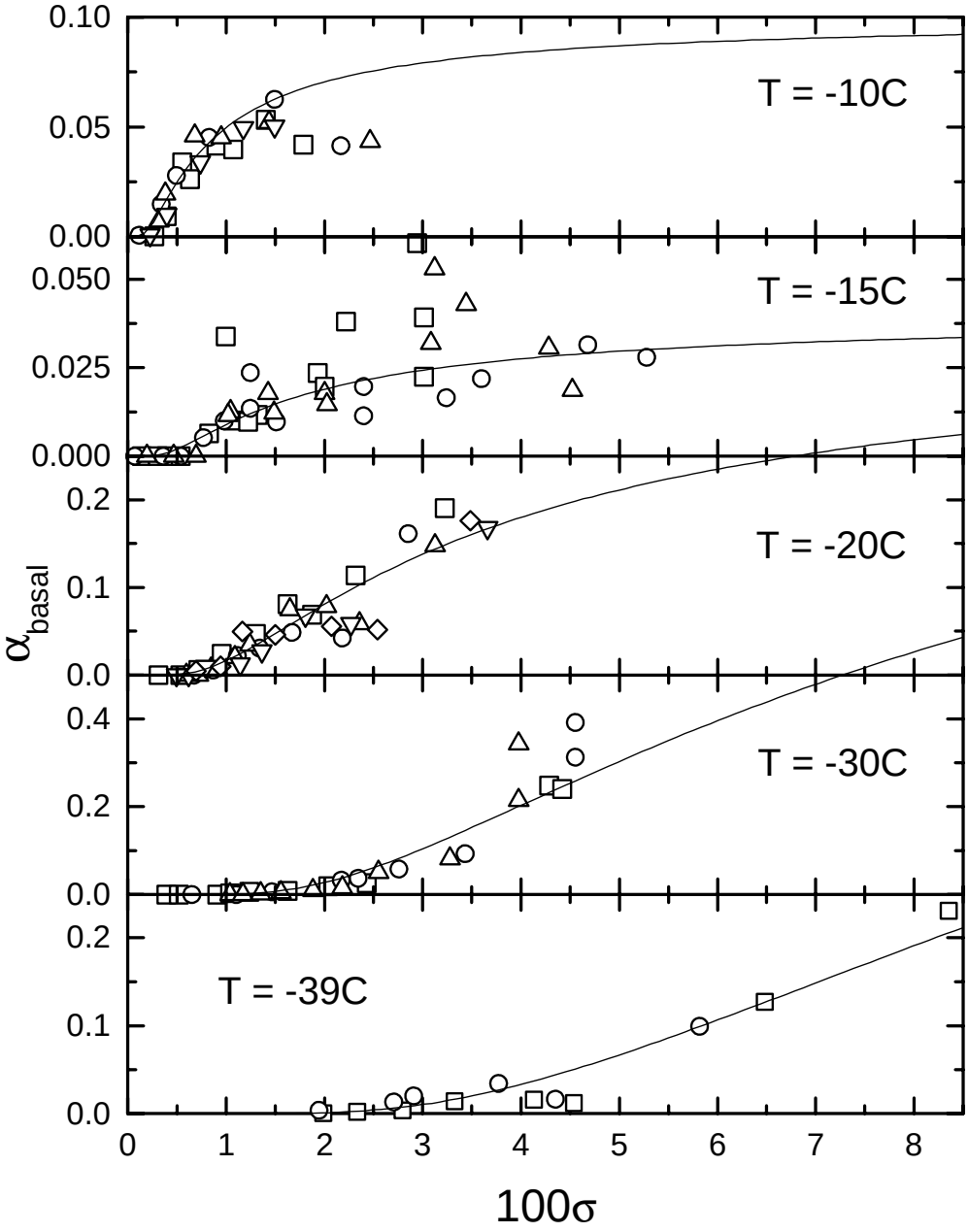

Figure 3. Measured condensation coefficients for the basal facets of ice crystals grown at different temperatures. Each set of symbols represents a series of growth velocity measurements made using a single crystal. The curves are fits to the data as described in the text. In this plot some of the $T = -39$ C data points lie outside the plot range.

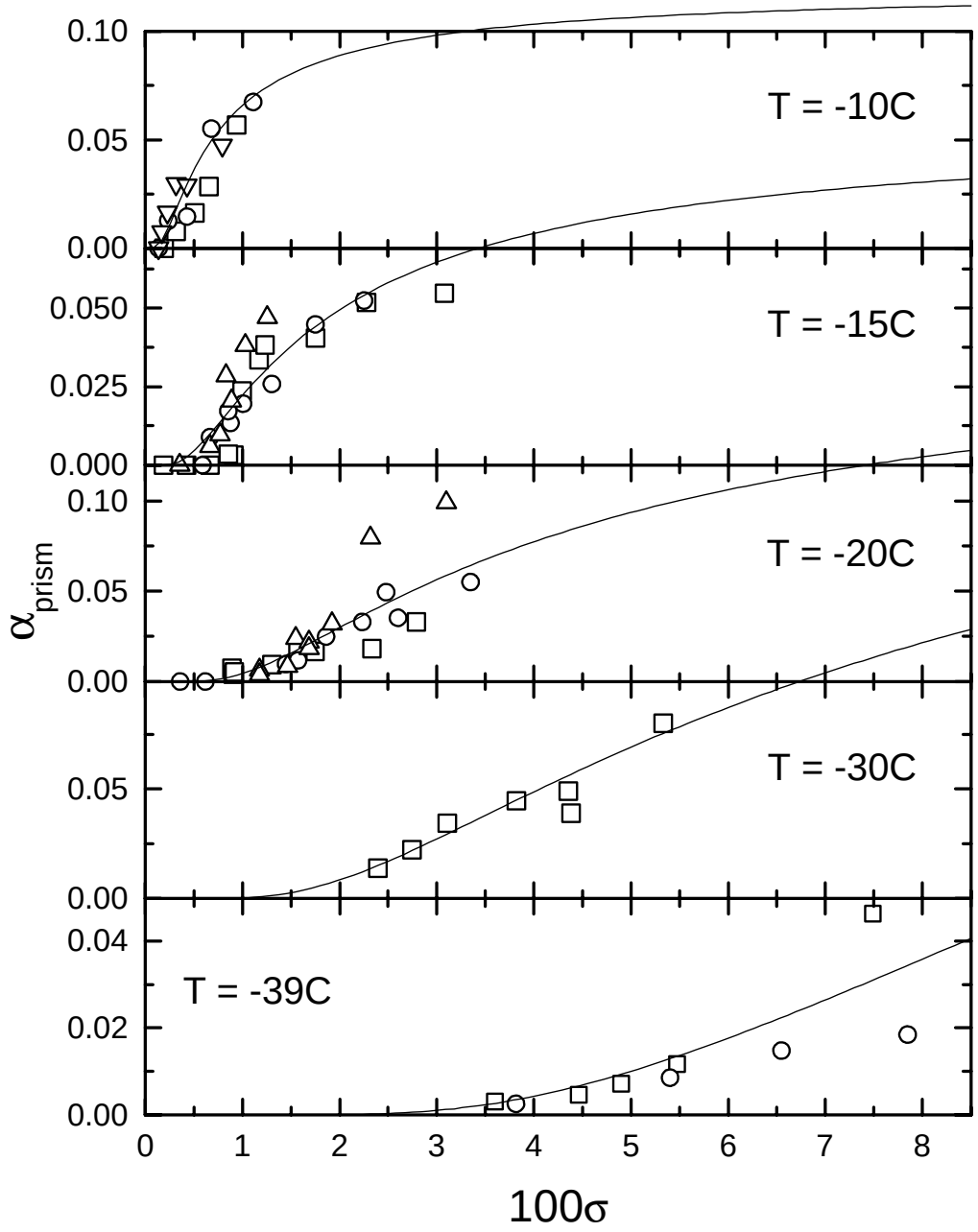

Figure 4. Measured condensation coefficients for the prism facets of ice crystals grown at different temperatures. Each set of symbols represents a series of growth velocity measurements made using a single crystal. The curves are fits to the data as described in the text. In this plot some of the $T = -39$ C data points lie outside the plot range.

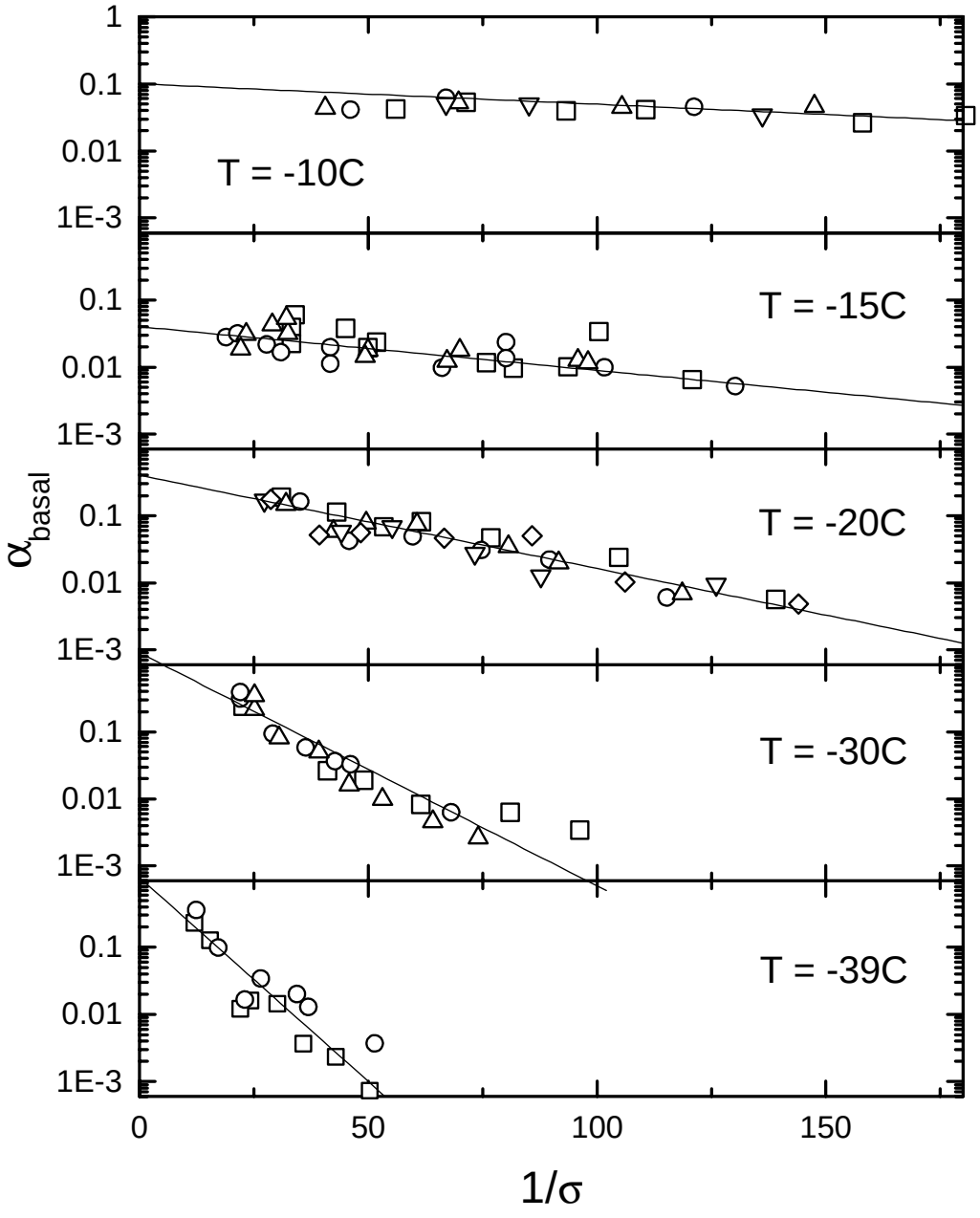

Figure 5. The same data as shown in Figure 3, replotted to show a linear trend when the growth is limited by 2D nucleation. In this plot some of the $T = -10$ C data points lie outside the plot range.

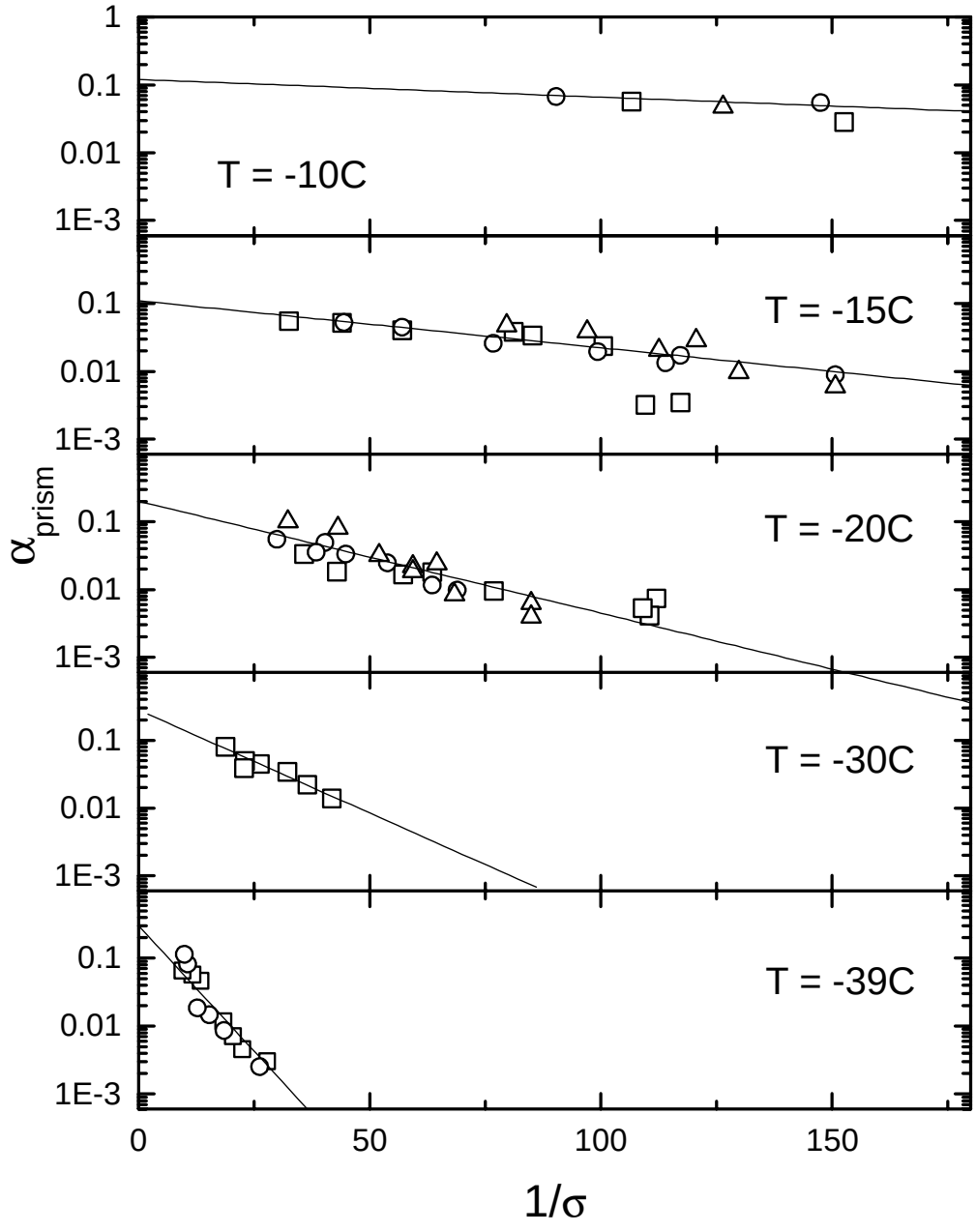

Figure 6. The same data as shown in Figure 4, replotted to show a linear trend when the growth is limited by 2D nucleation. In this plot some of the $T = -10$ C data points lie outside the plot range.

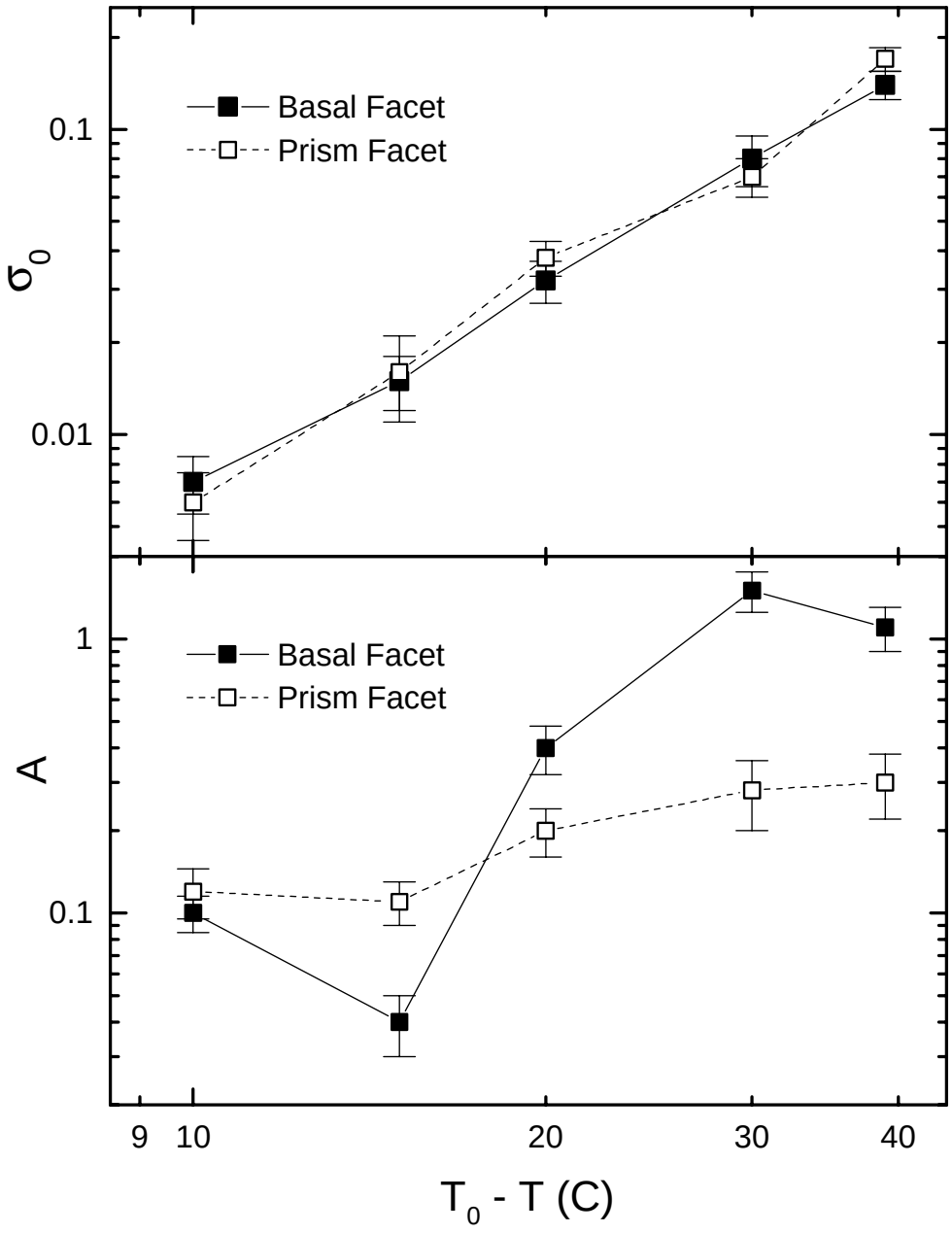

Figure 7. The fit coefficients $\sigma_0(T)$ and $A(T)$ as described in the text, where the condensation coeffiecient has been fit to the functional form $\alpha = A\exp(-\sigma_0/\sigma)$.

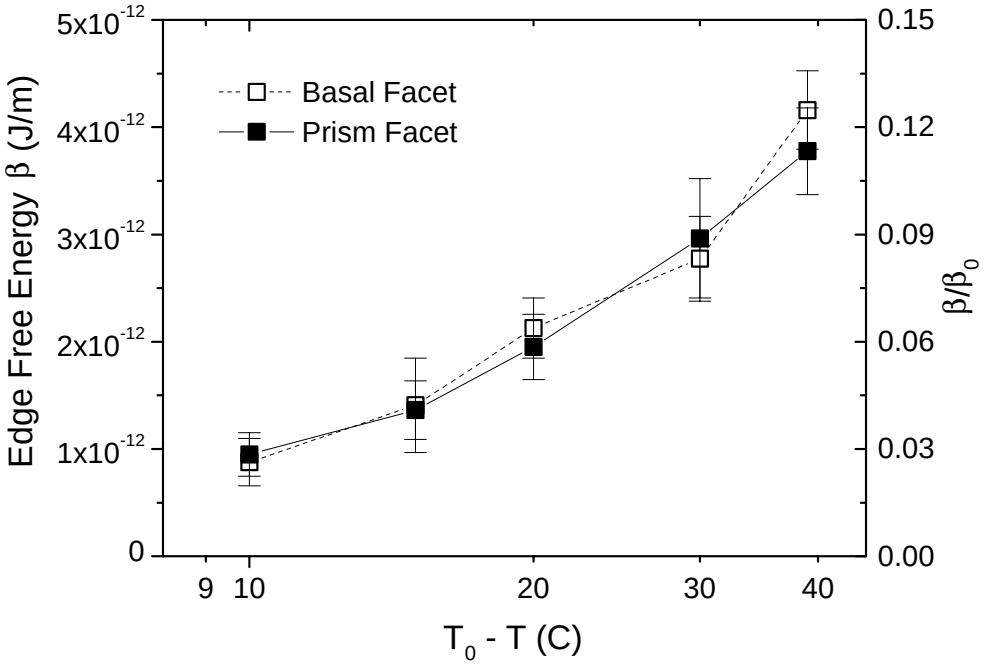

Figure 8. The edge free energy of a growing ice nucleus as a function of temperature, as derived from measurements of σ_0. The scale at right has been normalized by $\beta_0 = \gamma a$, where γ is the ice/vapor surface energy and a is the step height.